Design of a Folded Split Ring Resonator Antenna for Use in an Animal-Borne Sensor

S.C.K Dodson, P.G. Wiid, T.R. Niesler
Electrical & Electronic Engineering Department
University of Stellenbosch
Western Cape, South Africa
16522370@sun.ac.za, wiidg@sun.ac.za, trn@sun.ac.za

***Abstract*— We present the design, optimization and practical evaluation of a folded split ring resonator (FSRR) antenna for the purpose of radio communication with an animal-borne sensor. We show that measurements agree with the simulated results and that we are able to produce an antenna with small and adaptable physical dimensions, quasi-isotropic radiation pattern, low reflection coefficient and high radiation efficiency. We show that the FSRR is more suitable to other antennas commonly used for tracking. We conclude that this antenna is a feasible design for our application.**

I. INTRODUCTION

The conservation and study of endangered wildlife can be assisted by real-time information obtained from animal-borne sensors. We consider the case of the African rhinoceros, where the sensor will be mounted on its lower back leg. For wireless communication with the sensor, an antenna is required. The enclosure's small rectangular size of approximately $10\ mm \times 50\ mm \times 30\ mm$ makes the antenna's design challenging.

Little attention has been given to antenna design for tracking tags in the research literature. Usually, classic full-wave, half-wave and quarter-wave antennas are used. At our operating frequency, $f_0 = 433\ MHz$ these antennas must protrude from the enclosure to operate efficiently. This creates the risk of water leakage. The folded split ring resonator (FSRR) antenna provides a desirable alternative for its ability to operate efficiently within a small volume [1], inside the enclosure. We consider the design of this antenna, which is well matched to a $50\,\Omega$ line, has an approximately omnidirectional radiation pattern (quasi-isotropic) and a radiation efficiency e_{cd} that is close to unity.

II. THE FOLDED SPLIT RING RESONATOR

The FSRR is derived from a single-arm Split Ring Resonator (SRR). The SRR was conceived as a sub-wavelength metamaterial particle which has now seen extensive use as an electrically small antenna [2].

An electrically small antenna (ESA) is much smaller than the spherical boundary of its near-field. The boundary's radius is demarcated by its radianlength, $rl = \frac{\lambda}{2\pi}$, with λ the wavelength at the operating frequency. This is also the inverse of the free-space wave number $k = \frac{2\pi}{\lambda}$. An ESA's size is typically given relative to the radianlength by the ratio $\frac{a}{rl} = ka$ with a the radius of the smallest fictitious sphere that totally encloses the antenna.

The single-arm SRR, when fed at its center, may be interpreted as a half-wave dipole, curled into an electrically small circular shape, with a gap between the ends. The minimum radius, a, of the sphere enclosing a dipole decreases when the dipole is curled in this manner; the approximate decrease may be seen in Fig. 1 (a). Consequently, the radiation resistance R_{rad} lowers [3]. To mitigate this the curled dipole is folded. This adds an additional 'arm', increasing its input impedance by a factor of approximately four [4]. The conductor's circular cross-section is replaced by a planar one, allowing the antenna to be printed on a flexible substrate. The result is the FSRR antenna, shown in Fig. 1 (b).

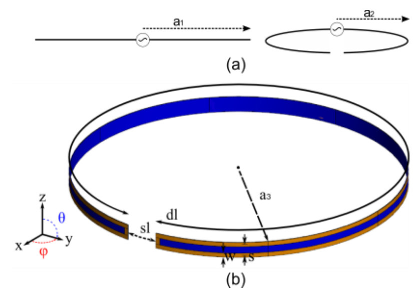

Fig. 1. (a) Half-wave dipole curled into SRR shape. (b) Computational model of the folded split ring resonator.

The electrically small size of the antenna causes the phase of the conductor currents (as well as the displacement current between the split gap) to be constant, producing a $\hat{z}$-directed magnetic dipole. Additionally, the opposite potentials along each arm create a $\hat{y}$-directed electric dipole. These combine to form a quasi-isotropic radiation pattern [1].

III. OPTIMISATION, CONSTRUCTION & RESULTS

The model in Fig. 1 was designed using the Method of Moments based computational electromagnetic software, FEKO on an FR-4 substrate with dielectric constant $\epsilon_r = 4.8$ and loss tangent $\tan\delta = 0.017$. It was optimized to most closely match a $50\ \Omega$ input impedance at $433\ MHz$. The split length sl, dipole length dl, conductor width w and spacing s were optimized; their values may be seen in Table I. The resulting size factor $ka = 0.47$ means the antenna can fit inside the enclosure if the circular form factor is modified to a rectangular one – this will be done in the future.

TABLE I. FSRR optimized parameters.

dl **[mm]**	***sl*** **[mm]**	***w*** **[mm]**	***s*** **[mm]**
31.58	10.40	1.38	3.53

A prototype was then constructed using a bazooka balun to choke unwanted common-mode currents occurring along the feed line [5]. The prototype is shown in Fig. 2. Measurements were made using the Agilent PNA-X 5242A Vector Network Analyzer and pattern measurements were conducted inside an anechoic chamber using a Spherical Near-Field Scanner.

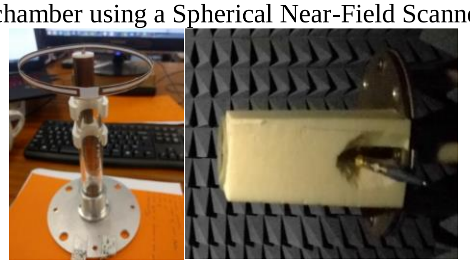

Fig. 2. Prototype of the FSRR on a flexible FR-4 substrate (left) and mounted in the anechoic chamber (right).

Fig. 3 shows measured and simulated values of the reflection coefficient (S_{11}) and indicates good agreement between the two. The minimum measured S_{11} value is -17.14 dB at 436.5 MHz. The $-10\ dB$ fractional bandwidth (FBW) is 1.9% (433 MHz − 441.40 MHz). The results indicate that the antenna will be well-matched at and above the desired operating frequency. Furthermore, the maximum simulated efficiency within the $-10\ dB$ FBW is 0.956 which is close to unity.

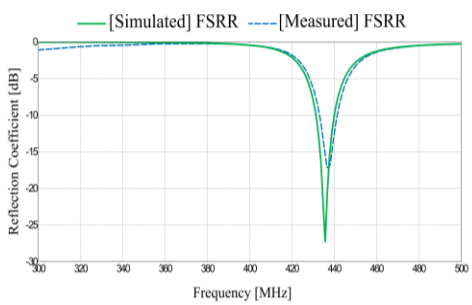

Fig. 3. Reflection coefficient of simulated FSRR versus the constructed prototype.

Far-field total directivity polar patterns are shown in Fig. 4. The plots show both measured and simulated traces. SNF scanner constraints cause inaccurate results for the independent θ scans between $90° < \theta < 270°$. The circular mounting plate seen in Fig. 2 acts as a scatterer, distorting the ideal pattern most notably in (a) and (b). When this plate is included in FEKO, there is a notable improvement in correspondence between the measured and simulated traces. We conclude from this agreement that when the plate is removed, the constructed antenna will radiate as predicted by the ideal trace (quasi-isotropically with a maximum directivity close to $1.25\ dB$, towards $\theta = 90°, \varphi = 0°$.) For comparison, a full-wave loop, half-wave dipole and quarter-wave monopole with a quarter-wave ground plane were simulated. The former two could conceivably wrap around the leg of the animal while the latter could extend from the enclosure. The dipole's S_{11} value was the lowest at $-15.03\ dB$, higher than the FSRR. However, its FBW is greater at 7.18%. Each antenna's e_{cd} is close to unity. These antennas lack the quasi-isotropic pattern and compact size of the FSRR. Given the narrow channel bandwidth the dipole's larger FBW is not essential. The FSRR is the appropriate choice for the application.

IV. Conclusion & Future Work

At $ka = 0.47$ the designed antenna fits into the prescribed enclosure. Early simulations where the antenna is bent into a rectangular form-factor to fit the enclosure indicate that the pattern is minimally affected. All plotted measurements agree with simulation results. The FBW is 1.9%, the far-field patterns show promising quasi-isotropic radiation behaviour which is desirable. Furthermore, the S_{11} value of $-17.14\ dB$ at and above the operating frequency is low. Finally, the antenna is desirable over common tracking antennas. The antenna is therefore a strong candidate for use in an animal-borne sensor.

Future prototypes will replace the bazooka balun with a surface mount balun. The antenna will be measured in the enclosure and compared to simulations. The radiation efficiency will be included in these measurements. A more compact planar model variation is being investigated. A phantom animal model is being developed in an adjacent project and will be incorporated if possible.

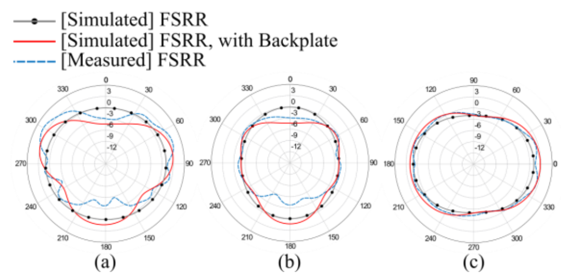

Fig. 4. Far-field polar plots showing total directivity of measured and simulated antenna, simulations with and without a 'plate', for (a) $\varphi = 0°$ varying θ, (b) $\varphi = 90°$ varying θ, (d) $\theta = 90°$ varying φ.

References

[1] J.-H. Kim and S. Nam, "A Compact Quasi-Isotropic Antenna Based on Folded Split Ring Resonators," *IEEE Antennas and Wireless Propagation Letters*, pp. 1–1, 2016.

[2] Yuandan Dong and T. Itoh, "Metamaterial-Based Antennas," *Proceedings of the IEEE*, vol. 100, no. 7, pp. 2271–2285, Jul. 2012.

[3] H. A. Wheeler, "Fundamental limitations of small antennas," *Proceedings of the IRE*, vol. 35, no. 12, pp. 1479–1484, 1947.

[4] C. A. Balanis, *Antenna theory: analysis and design*, 3. ed. Hoboken, NJ: Wiley-Interscience, 2005.

[5] S. A. Saario, J. W. Lu, and D. V. Thiel, "Full-wave analysis of choking characteristics of sleeve balun on coaxial cables," *Electronics Letters*, vol. 38, no. 7, pp. 304–305, 2002.